Article:
Du, X, Liu, Y, Wang, F et al. (2021) A Fluorescence Sensor for Pb2+ Detection Based on Liquid Crystals and Aggregation-Induced Emission Luminogens. ACS Applied Materials & Interfaces, 13 (19). pp. 22361-22367. ISSN: 1944-8244

https://doi.org/10.1021/acsami.1c02585

Fluorescence sensor for Pb^{2+} detection based on liquid crystals and aggregation-induced emission luminogen

Xiaoxue Du,[1, 2] Yanjun Liu,[1] Fei Wang,[1] Dongyu Zhao,[3,] Helen F. Gleeson[2,*] and Dan Luo[1,*]*

[1] Department of Electrical and Electronic Engineering, Southern University of Science and Technology, Shenzhen, 518055, China

[2] School of Physics and Astronomy, University of Leeds, Leeds, LS2 9JT, UK

[3] School of Chemistry and Environment, Beihang University, Beijing, 100191, China

* zhaodongyu@buaa.edu.cn

* h.f.gleeson@leeds.ac.uk

* luod@sustech.edu.cn

KEYWORDS: lead ions, liquid crystals, aggregation-induced emission, biological sensing and sensors, DNAzyme

ABSTRACT: Heavy metals, such as lead ions, are regarded as the main environmental contaminants and have a negative impact on human bodies, making detection technologies of lead ions critical. However, most existing detection methods suffer from time consuming, complicated sample pre-treatment, and expensive equipment, which hinder their broad use in

real-time detection. Herein, we show a new fluorescent sensor for detecting lead ions derived from liquid crystals doped with an aggregation-induced emission luminogen. The mechanism is based on the variation of fluorescence intensity caused by the disturbance of an ordered liquid crystal configuration in presence of Pb^{2+}, induced by DNAzyme and its catalytic cleavage. The proposed fluorescence sensor exhibits a low detection limit of 0.65 nM, which is two orders of magnitude lower than that previously reported in an optical sensor based on liquid crystal. The detection range of the Pb^{2+} fluorescence sensor is broad, from 20 nM to 100 μM, and it also select lead ion from numerous metal ions exactly, resulting in a highly sensitive, highly selective, simple and low-cost detection strategy of Pb^{2+} with potential applications in chemical and biological fields. This approach to designing a liquid crystal fluorescence sensor offers an inspiring stage for detecting biomacromolecule or other heavy metal ions by varying decorated molecules.

INTRODUCTION

Lead ions, as major heavy metal in environmental pollutants, are harmful to human health and can lead to problems such as muscle paralysis, anemia, memory loss, and mental health concerns.[1,2] Several technologies have been proposed to detect lead ions such as plasma atomic emission spectroscopy,[3] atomic absorption spectroscopy,[4] surface enhanced Raman spectroscopy,[5] colorimetric,[6,7] quantum dots,[8,9] electrochemical,[10] and biochemical[11] methods. However, those analytical methods usually require large or expensive equipment with sophisticated operators, complicated operation processes, and time-consuming sample pre-treatments, thus developing a novel strategy for Pb^{2+} real-time detection is highly desirable.

Liquid crystals are substances that flow like the liquid but remain some of the ordering properties of crystals, which have anisotropy properties. In the liquid crystal phase, the

molecule's preferred orientation, *n*, is regarded as the “director”. The long axes of the molecules will be inclined to align in this direction. The macroscopic orientation of the director can be influenced by external electric fields, external magnetic fields, surface treatments, chiral agents. Recently, liquid crystal (LC) based optical biochemical sensors[12-14] sensors have attracted considerable attention due to the extraordinary sensitivity of chemical and physical properties at a bounding interface that can transduce molecular events to a bulk response.[15-17] LC based optical sensors for the detection of protein and cancer cells,[18] polymer chemicals,[19] bacteria,[20] viruses,[21] and mercuric ions[22] have been designed with features including low-cost, simplicity and rapid responses. Moreover, many studies have reported the DNA functionalized sensing systems, including “8-17” DNAzyme,[23,24] quadruplex DNAzyme,[25] and GR-5 DNAzyme. [26,27] Further, a novel naked-eye optical sensor based on LCs decorated with DNAzyme for the detection of lead ions was recently reported by our group.[23] The LC sensor described in that work owns a particularly wide range detection of lead ions (50 nM ~ 500 μM). However, the limit of detection is approximately 36.8 nM, which is unsatisfactory. Therefore, it is highly desirable to improve the limit of detection of the LC sensor for Pb^{2+} while maintaining the broad detection range.

In this letter, we report a liquid crystal fluorescence sensor developed for Pb^{2+} detection derived from liquid crystals doped with an aggregation-induced emission (AIE) luminogen. The mechanism is based on the variation of the fluorescence intensity caused by the disturbance of the liquid crystal configuration due to the existence of Pb^{2+}, induced by DNAzyme and its catalytic cleavage. The proposed fluorescence sensor reveals a low detection limit as well as a broad detection range, leading to a highly sensitive, highly selective, simple, and low-cost

detection strategy for Pb^{2+}. This device can be applied in environmental monitoring, industry process monitoring, and clinical toxicology with great potential.

Aggregation-induced emission is an extraordinary photophysical phenomenon that is the opposite of aggregation-induced quenching, where the AIE fluorogens are highly emissive in aggregation due to the restriction of rotation within the molecular.[28-30] This materials have attracted significant attention in various fields such as luminescent materials,[31] sensors,[32] bioimaging,[33] biology delivery,[34] and theranostics.[35,36] Several research works have been reported that combine AIE materials with liquid crystals, such as the work by Zhao who demonstrated light-emitting liquid crystal displays and reported their performance under electric field, based on an AIE luminogen obtained through synthesizing an AIE-LC material.[37-39] It is expected that AIE luminogens will enable fluorescent LC based sensors and largely decrease the limit of detection in the probes, comparing to previously naked-eye based LC sensors.

MATERIALS AND METHODS

H_2O_2, H_2SO_4, dimethyloctadecyl [3-(trimethoxysilyl) propyl] ammonium chloride (DMOAP), (3-Aminopropyl) triethoxysilane (APTES), C_2H_5OH, glutaral (GA), dodecyl trimethyl ammonium bromide (DTAB), $Pb(NO_3)_2$, $CuCl_2$, $ZnCl_2$, $AgNO_3$, $CdCl_2$, $MgCl_2$, $MnCl_2$ and KCl were purchased from Sigma-Aldrich (St. Louis, USA). The nematic liquid crystals 4-cyano-4'-pentylbiphenyl (5CB) was purchased from HCCH (Jiangsu China). The DNAzyme were obtained from Shenggong Bioengineering (Shanghai, China). Dongsheng Glass (Taizhou, China) provided the glass slides (Sail brand). The TPE-PPE (tetraphenylethylene-propylphenylethyne), as the AIE material here, was supplied by Beihang University. The chemical structures of 5CB, DTAB, APTES, GA, TPE-PPE and DMOAP are shown in Figure 1a. The samples' images were captured by optical microscope (Ti200, Nikon). The fluorescence

intensity was obtained from processing the images, which were captured by a charge coupled device (CCD) camera (Nikon Ds-Ri2), where the gamma correction coefficient of the CCD was 1 and the integration time was 200 ms. The fluorescence spectrum was obtained by microspectrophotometer (CRAIC technologies Inc.). The Milli-Q water purification system (Millipore, Bedford, MA) was operated to prepare all aqueous solutions with deionized water (DI water).

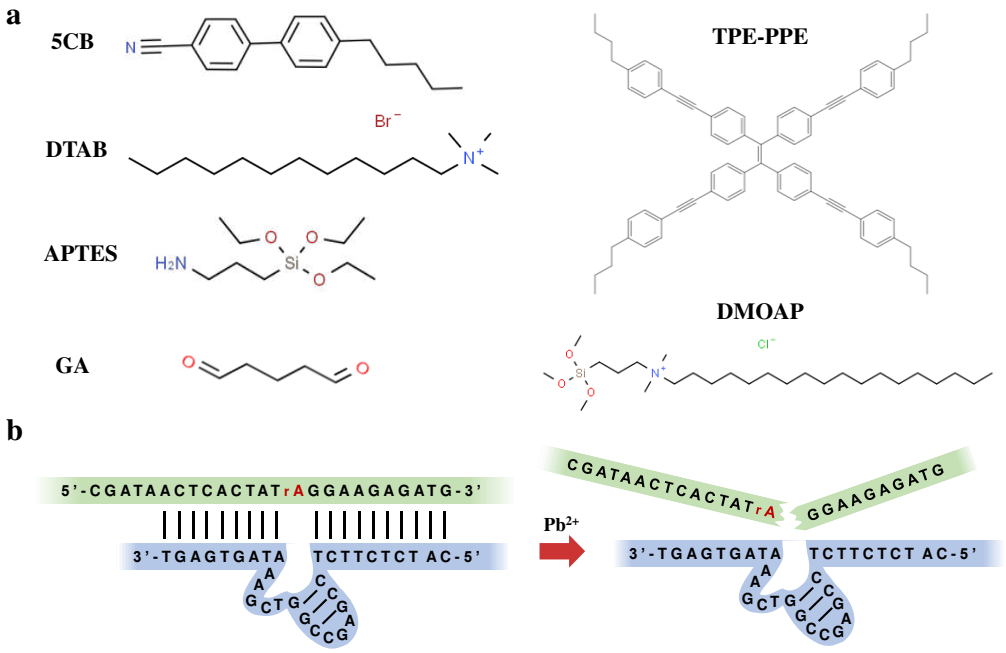

Figure 1. (a) Chemical structures of 5CB, DTAB, APTES, GA, TPE-PPE and DMOAP for lead ion fluorescence sensor. (b) Schematic illustration of catalytically cleave of complementary DNA molecules.

The process of substrate's pretreatment and anchoring operations are the same as those in our previous work on the optical sensor based on liquid crystal and DNAzyme.[23] More preparation details can be checked in [Ref 23]. The substrate was treated with sufficient piranha solution and then washed with plenty of DI water. Then it was dried with N_2 and soaked in an ethanol solution containing DMOAP and APTES. The anchoring of 5CB was indeed influenced

by the DMOAP. For this sensor, the DMOAP was bonded to the substrate because of the covalent Si-O-Si bonds. The carbon chain units on the other side of the "Si" kept vertical and induced the liquid crystals to vertically align on glass substrate. The APTES molecules, which has terminal amino groups capable of attracting anionic complementary DNA strands (base sequence and structure corresponded to Figure 1b). The strands consisted of a catalytic strand and its combined strand, attaching on the glass substrate through covalent bonds (Si-O-Si). GA was subsequently applied to the surface and dried. Then, the catalytic strands (200 μM) and combined strands (200 μM) were combined to this system. GA acted as the intermediate through the amino groups between APTES and DNA strand. Next, the unbonded DNA strands of sample were washed by DI water. Transmission electron microscopy (TEM) grids (copper mesh) were then put on the glass substrate. After that, 1 μL of solution mixed with 5CB (99.9 wt%) and TPE-PPE (0.1 wt%) was distributed onto the grid. Finally, the TEM grid was placed in DTAB environment. The electrostatic interaction linked DTAB molecules to the DNA and this led to a good dissolution of DNA through a self-assembled monolayer at the LC/aqueous interface. Therefore, on the bottom glass substrate, the DMOAP was applied to help the LC molecules be in a homeotropic alignment. On the top interface of LC and aqueous solution, the DTAB also aligned LC molecules vertically. Based on both vertically alignments of DMOAP and DTAB, a homeotropic configuration of LC was achieved.[7] The DNAzyme is a kind of 8-17 DNAzyme, which is a mature and popular choice that corresponding to lead ion[24]. The DNAzyme would be disassembled because of catalytic cleavage at the "rA" site of DNA molecules, as shown in Figure 1b. The thickness of the TEM grid was 10 μm and all experiments were finished at room temperature (25 ^{o}C). The orientation of AIE featured TPE-PPE obtained a perpendicular orientation in the homeotropic LC mixture.[37] It is worth noticing that the orientation of AIE-

featured TPE-PPE was induced by the orientation nematic liquid crystal 5CB here. Therefore, the liquid crystal molecules and AIE molecules were anchored by these vertical long chains formed by DMOAPAPTES-GA-DNA-DTAB on glass substrate[7,23]. The homeotropic configuration of LC/AIE was formed through self-assembly property of LC molecules.

In our experiment, the sensor was placed under an optical microscope to capture the fluorescence signal, and was stimulated by an ultraviolet (UV) light (365 nm). Figure 2 depicts the process of Pb^{2+} sensing in the AIE doped LC optical sensor. The AIE-featured TPE-PPE molecules aggregate in the nematic liquid crystal mixture at a concentration of 0.1 wt% in our experiment, which leads to a significantly high fluorescence efficiency.[37] According to quantum chemistry calculations, the emission dipole moment of TPE-PPE is parallel to the double bond.[38] The dipole moment along the short axis direction is greater than that along the long axis direction of TPE-PPE molecule, leading to a stronger fluorescence of molecules for a homeotropic configuration when observed using optical microscopy.[39] Initially, the liquid crystal 5CB molecules (and DNA strands) possess a vertical alignment configuration (homeotropic configuration) on the glass substrate with DMOAP, which forms homeotropic configuration and induces vertically alignment of AIE-featured TPE-PPE (as shown in the left part of Figure 2). The corresponding florescence intensity of sample under UV illumination is relatively high. In the presence of lead ions, the complementary DNA strand disassembles based on catalytic cleavage of DNA, which disturbs the vertical alignment of LC (5CB) as well as AIE-featured TPE-PPE (as shown in the right part of Figure 2), resulting in a relatively low florescence intensity of sample under UV illumination. It is worth noticing that the orientation of AIE-featured TPE-PPE is induced by the orientation nematic liquid crystal 5CB here, thus leading to

the fluorescent intensity change, which is different from the ordinary AIE where the fluorescent intensity change is due to the aggregation of AIE molecules.

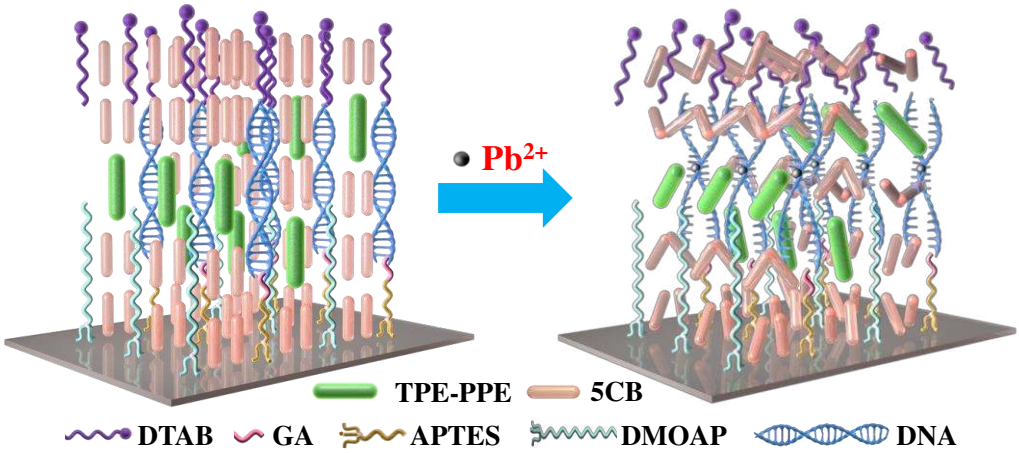

Figure 2. Schematic illustration of the sensing system on the basis of liquid crystals doped with AIE for detecting lead ions.

RESULTS AND DISCUSSION

The concentration of DTAB is critical for liquid crystal alignment with DNA molecules in the initial homeotropic configuration. The fluorescence image of the Pb^{2+} sensor under illumination by UV light (365 nm, 5.6 mW/cm^2) is shown in Figure 3, for concentrations of DTAB varying from 0 μM to 50 mM without the presence of Pb^{2+}. It can be seen that, without DTAB (0 μM) the fluorescence intensity of sample is low, leading to a relatively dark fluorescent image (Figure 3a). The brightness increases with increasing concentration of DTAB (Figures 3b-3d), suggesting that more AIEgens are anchored on the glass slide vertically. The fluorescence image tends to saturate when DTAB's concentration reaches 10 mM, above which there is no further significant change in the brightness of sample. The saturation of the alignment effect of DTAB is accompanied by the anion-cation balance originating from the cationic in DTAB and anionic in the complementary DNA strand. In our following experiments, the

optimum concentration of DTAB was chosen to be 10 mM. Figure 3 plots the relationship of DTAB concentration and the fluorescence intensity.

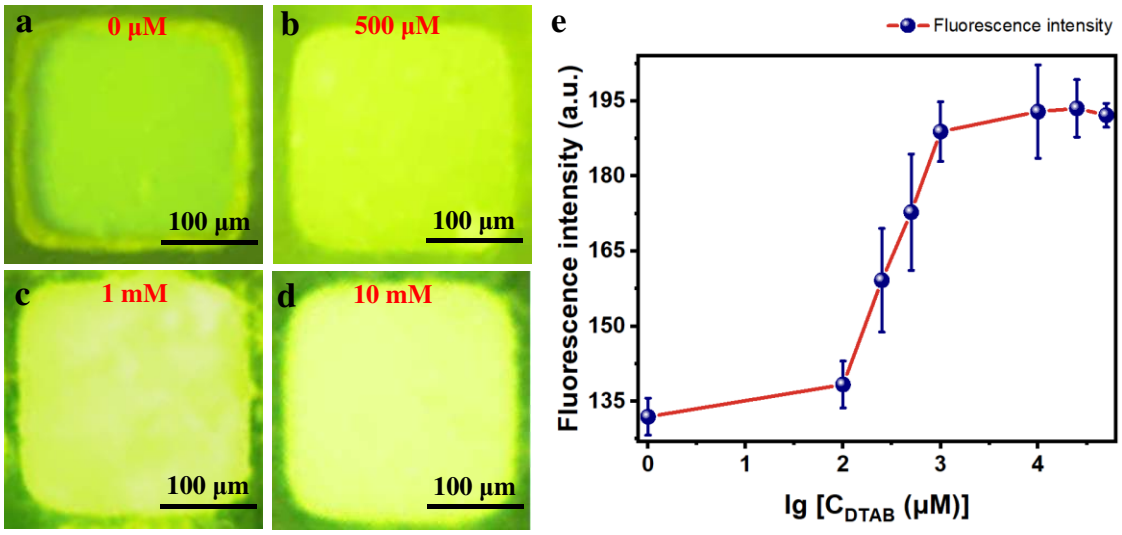

Figure 3. Fluorescence image of the lead ion sensor sample viewed by optical microscopy with the concentration of DTAB varying from (a) 0 μM, (b) 500 μM, (c) 1 mM, (d) 10 mM, without the presence of Pb^{2+}. (e) The relationship of DTAB concentration and the fluorescence intensity. The scale bar is 100 μM.

The influence of lead ions' concentrations on the luminance of sensor's fluorescence was studied to provide a quantitative analysis. Figure 4a-4h show fluorescence images of the Pb^{2+} sensor under illumination by UV light at am intensity of 6.7 mW/cm^2, for varying concentrations of Pb^{2+} (from $Pb(NO_3)_2$) solution (0 nM - 100 μM). The initial fluorescence image, without Pb^{2+}, is shown in Figure 4a, demonstrating a highly brightness. Herein, the AIE molecules were anchored on the glass slide vertically with the homeotropic configuration of LC molecules. During the process of adding Pb^{2+}, the DNA molecules are catalytically cleaved, disturbing the orientation of both the liquid crystal and AIEgens, resulting in a darker fluorescence in the sensor. The concentration of added Pb^{2+} determined the amount of cleavage of the DNA strands; increasing the Pb^{2+} concentration caused more DNA strands to be cleaved, leading to a darker

sensor. The response time is counted with starting time of adding Pb2+ on the sensor and ending time of viewing stable fluorescence in optical microscope. The response time of Pb^{2+} sensor was less than 20 seconds. Figure 4i plots the absorption spectra of our sensor before and after adding 1 μM Pb^{2+}. It is clear that there is no obvious difference between the two spectra. Figure 4j shows the emission spectra of our sensor before and after 1 μM Pb^{2+} added, where the central wavelength is unchanged while the intensity dramatically decreases after addition of 1 μM Pb^{2+}.

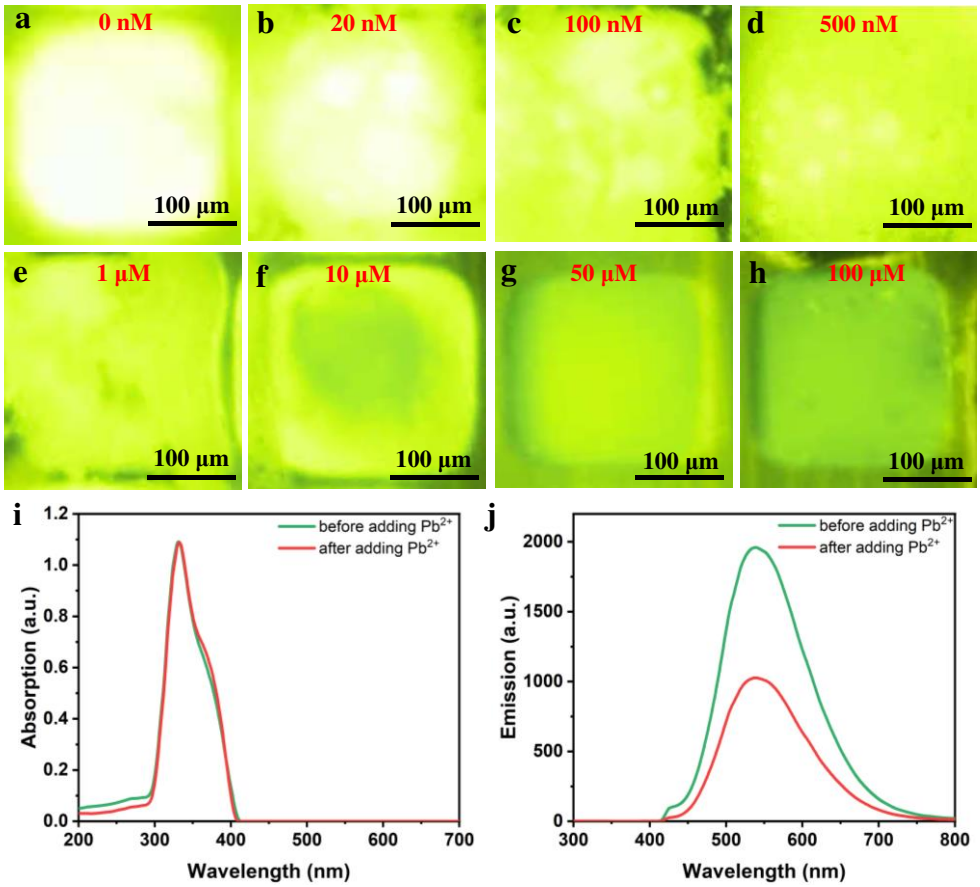

Figure 4. The fluorescence images of the sensor observed using a microscope where the concentration of Pb^{2+} is (a) 0 nM, (b) 20 nM, (c) 100 nM, (d) 500 nM, (e) 1 μM, (f) 10 μM, (g) 50 μM, and (h) 100 μM. The scale bar is 100 μm. (i) Absorption spectrum of our sensor before and after adding 1 μM Pb^{2+}. (j) Emission spectrum of our sensor before and after adding 1 μM Pb^{2+}.

Figure 5 plots the relationship of Pb^{2+} concentration and the fluorescence intensity of the sensor. Within the detection range, from 20 nM to 100 μM, the fluorescence intensity varies from very bright to relatively dark. This sensor is relative stable and not very sensitive to the environmental temperature within 15 ºC ~ 30 ºC. After processing the images from multiple samples under the same conditions, the average intensity, *I*, and standard deviation were determined for each Pb^{2+} concentration was measured and fitted to the relationship $I = -26.98(\ln C_{Pb^{2+}}) + 237.1$ with a correlation coefficient of R^2=0.9918 ($C_{Pb^{2+}}$ is the concentration of Pb^{2+} in nM).

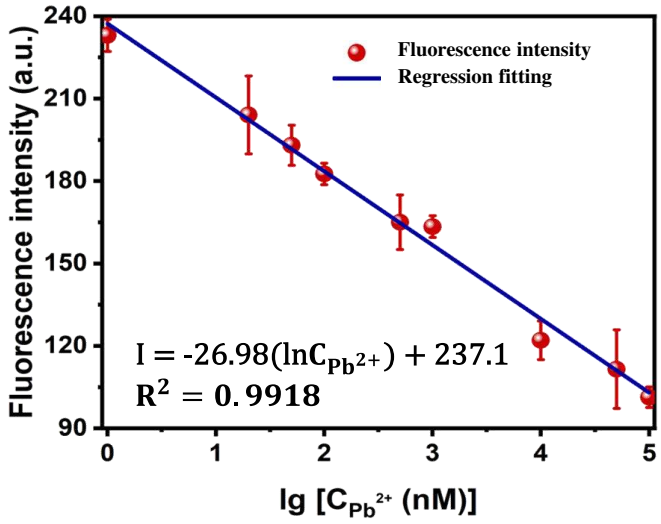

Figure 5. The relationship of Pb^{2+} concentration and the fluorescence intensity of sensor.

According to the theory of Martins and Naes,[33] the limit of detection (LOD) with the rule of 3σ/slope (σ refers to the standard deviation of the background obtained from multiple measurements in blank samples) can be worked out as 0.65 nM, which is two orders of magnitude lower than previously reported result of 36.8 nM from liquid crystal based Pb^{2+} optical sensor.[27] It can compare with those of sensors based on organic dye and quantum dots (from 0.1 nM-0.6 nM).[41-43] In addition, the detection range (20 nM-100 μM) of this proposed strategy is rather wider than those based on organic dyes (2-50 nM),[41] semiconductor quantum

dots (0.1-10 nM),[42] graphene quantum dots/graphene oxide (9.9-435.0 nM),[43] and graphene quantum dots/gold nanoparticles (50 nM-4 μM).[44] The comparison of these related Pb^{2+} sensors are shown in Table 1. The broad detection range with high sensitivity of our sensor is critical for its practical applications.

Table 1. The comparison of related Pb^{2+} sensors

Methods	**Materials**	**LOD**	**Linear range**	**References**
Fluorescent	GR-5 DNAzyme, nanoparticles	1.108 nM	0-1 nM	Ref 27
Fluorescent	G-quadruplex DNA, graphene oxide	0.4 nM	2-50 nM	Ref 41
Fluorescent	CdSe/ZnS quantum dots, graphene oxide	0.09 nM	0.1-10 nM	Ref 42
Fluorescent	Graphene quantum dots-aptamer probe, graphene oxide	0.6 nM	9.9-435.0 nM	Ref 43
Fluorescent	Graphene quantum dots, gold nanoparticles	16.7 nM	50 nM-4 μM	Ref 44
Gray-value	8-17 DNAzyme, LC	36.8 nM	50 nM-500 μM	Ref 23
Fluorescent	8-17 DNAzyme, LC, AIE	0.65 nM	20 nM-100 μM	Our work

The selectivity is also a critical indicator for sensor. Figure 6 plots the performance of the sensor at 1 μM Pb^{2+} and 100 μM Cu^{2+}, Zn^{2+}, Ag^{+}, Cd^{2+}, Mg^{2+}, Mn^{2+} and K^{+}. The initial and final fluorescence is denoted by F_i and F_f, respectively. The ratio of the change in fluorescence intensity is determined by $(F_i - F_f)/ F_i$. It is obviously that the change of fluorescence intensity is significant on adding 1 μM Pb^{2+} to the sensor, while effectively no change occurs in the presence of other metal ions with the concentration of 100 μM. About three times the value of influence of lead ions was achieved in comparison to other metal ions. The results indicate that only Pb^{2+} ions can cleave the DNAzyme strands, thus disrupting the homeotropic configuration of the LC and the AIE materials TPE-PPE. This fluorescence sensor shows a negligible response to Cu^{2+}, Zn^{2+},

Ag^{+}, Cd^{2+}, Mg^{2+}, Mn^{2+} and K^{+} under similar condition. Due to the reason that double stranded DNA with C or G bases in addition of sufficient Ag^{+} can form Ag^{+}-mediated guanine pairing,[45] the anchoring of the sensing system would be affected slightly. Therefore, the Ag^{+} had a higher fluorescence changing ratio compared to other ions.

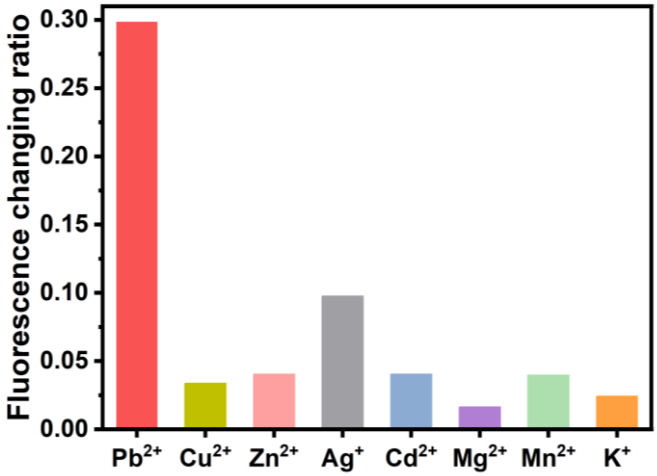

Figure 6. Selectivity of the fluorescence sensor under existing of 100 µM Cu^{2+}, Zn^{2+}, Ag^{+}, Cd^{2+}, Mg^{2+}, Mn^{2+}, K^{+} and 1 µM Pb^{2+}.

CONCLUSION

In this study, a fluorescence sensor for detecting lead ions on the basis of AIE-doped liquid crystals has been demonstrated. A disordered configuration of the liquid crystal sample doped with AIE luminogen leads to reduction in the fluorescence intensity, which is led by catalytic cracking of complementary DNA strand in existing of Pb^{2+}. The proposed fluorescence sensor possesses a low LOD of 0.65 nM, which is two orders of magnitude lower than that from previously reported LC optical sensor. The detection range of the Pb^{2+} fluorescence sensor is broad, from 20 nM to 100 µM. It also indicates that this sensor can select Pb^{2+} from many other metal ions correctly, resulting in a highly sensitive, highly selective, simple and low-cost detection strategy for Pb^{2+} with potential applications in chemical and biological fields. This LC

fluorescence sensor can provide an inspiring platform for detection by varying the decorated molecules, such as detecting other heavy metal ions and antigens.

ACKNOWLEDGEMENTS

This work is supported by Natural National Science Foundation of China (NSFC) (61875081, 51973007), Shenzhen Science and Technology Innovation Commission (JCYJ20180305180700747), Beijing Natural Science Foundation of China (2192030), and Engineering and Physical Sciences Research Council (EP/P024041/1).

REFERENCES AND LINKS

(1) Lee, H. Y.; Bae, D. R.; Park, J. C.; Song, H.; Han, W. S.; Jung, J. H. A Selective Fluoroionophore Based on BODIPY-Functionalized Magnetic Silica Nanoparticles: Removal of Pb^{2+} from Human Blood. *Angew. Chem., Int. Ed.* **2009,** 48, 1239–1243.

(2) Sebastian, M.; Mathew, B. Ion Imprinting Approach for the Fabrication of an Electrochemical Sensor and Sorbent for Lead Ions in Real Samples Using Modified Multiwalled Carbon Nanotubes. *J. Mater. Sci.* **2018,** 53, 3557–3572.

(3) Zheng, C. B.; Hu, L. G.; Hou, X. D.; He, B.; Jiang, G. B. Headspace Solid-Phase Microextraction Coupled to Miniaturized Microplasma Optical Emission Spectrometry for Detection of Mercury and Lead. *Anal. Chem.* **2018,** 90, 3683–3691.

(4) Wang, Y. K.; Gao, S. T.; Zang, X. H.; Li, J. C.; Ma, J. J. Graphene-Based Solid-Phase Extraction Combined with Flame Atomic Absorption Spectrometry for a Sensitive

Determination of Trace Amounts of Lead in Environmental Water and Vegetable Samples. *Anal. Chem. Acta.* **2012,** 716, 112–118.

(5) Shi, X. H.; Gu, W.; Zhang, C. L.; Zhao, L. Y.; Li, L.; Peng, W. D.; Xian, Y. Z. Construction of a Graphene/Au-Nanoparticles/Cucurbit[7]uril-Based Sensor for Pb^{2+} Sensing. *Chem. Eur. J.* **2016,** 22, 5643–5648.

(6) Kim, H. N.; Ren, W. X.; Kim, J. S.; Yoon, J. Fluorescent and Colorimetric Sensors for Detection of Lead, Cadmium, and Mercury Ions. *Chem. Soc. Rev.* **2012,** 41, 3210–3244.

(7) Huang, Z. J.; Chen, J. M.; Luo, Z. W.; Wang, X. Q.; Duan, Y. X. Label-Free and Enzyme-Free Colorimetric Detection of Pb^{2+} Based on RNA-Cleavage and Annealing-Accelerated Hybridization Chain Reaction. *Anal. Chem.* **2019,** 91, 4806–4813.

(8) He, Z. Q.; Zhang, C. C.; Dong, Y. J.; Wu, S. T. Emerging Perovskite Nanocrystals-Enhanced Solid-state Lighting and Liquid-crystal Displays. *Crystals* **2019,** 9, 59.

(9) He, Z. Q.; He, J.; Zhang, C. C.; Wu, S. T.; Dong, Y. J. Swelling Deswelling Microenca Fpsulation Enabled Ultrastable Perovskite−Polymer Composites for Photonic Applications. *Chem. Rec.* **2020,** 20, 672–681.

(10) Wang, Y. G.; Zhao, G. H.; Zhang, Q.; Wang, H.; Zhang, Y.; Cao, W.; Zhang, N.; Du, B.; Wei, Q. Electrochemical Aptasensor Based on Gold Modified Graphene Nanocomposite with Different Morphologies for Ultrasensitive Detection of Pb^{2+}. *Sens. Actuators, B* **2019,** 288, 325–331.

(11) Li, T.; Dong, S. J.; Wang, E. A lead (II)-Driven DNA Molecular Device for Turn-on Fluorescence Detection of Lead (II) Ion with High Selectivity and Sensitivity. *J. Am. Chem. Soc.* **2010,** 132, 13156–13157.

(12) Wang, X.; Miller, D. S.; Bukusoglu, E.; de Pablo, J. J.; Abbott, N. L. Topological Defects in Liquid Crystals as Templates for Molecular Self-Assembly. *Nat. Mater.* **2016,** 15, 106–112.

(13) Iino, H.; Usui, T.; Hanna, J. Liquid Crystals for Organic Thin-Film Transistors. *Nat. Commun.* **2015,** 6, 6828.

(14) Sivakumar, S.; Wark, K. L.; Gupta, J. K.; Abbott, N. L.; Caruso, F. Liquid Crystal Emulsions as the Basis of Biological Sensors for the Optical Detection of Bacteria and Viruses. *Adv. Funct. Mater.* **2009,** 19, 2260–2265.

(15) Shah, R. R.; Abbott, N. L. Principles for Measurement of Chemical Exposure Based on Recognition-Driven Anchoring Transitions in Liquid Crystals. *Science* **2001,** 293, 1296–1299.

(16) Price, A. D.; Schwartz, D. K. DNA Hybridization-Induced Reorientation of Liquid Crystal Anchoring at the Nematic Liquid Crystal/Aqueous Interface. *J. Am. Chem. Soc.* **2008,** 130, 8188–8194.

(17) He, Z. Q.; Tan, G. J.; Chanda, D.; Wu, S. T. Novel Liquid Crystal Photonic Devices Enabled by Two-photon Polymerization. *Opt. Express* **2019,** 27, 11472-11491.

(18) Yoon, S. H.; Gupta, K. C.; Borah, J. S.; Park, S. Y.; Kim, Y. K.; Lee, J. H.; Kang, I. K. Folate Ligand Anchored Liquid Crystal Microdroplets Emulsion for in Vitro Detection of KB Cancer Cells. *Langmuir* **2014,** 30, 10668–10677.

(19) Manda, R.; Dasari, V.; Sathyanarayana, P.; Rasna, M.; Paik, P.; Dhara, S. Possible Enhancement of Physical Properties of Nematic Liquid Crystals by Doping of Conducting Polymer Nanofibres. *Appl. Phys. Lett.* **2013,** 103, 141910.

(20) Cadwell, K. D.; Alf, M. E.; Abbott, N. L. Infrared Spectroscopy of Competitive Interactions Between Liquid Crystals, Metal Salts, and Dimethyl Methylphosphonate at Surfaces. *J. Phys. Chem. B* **2006,** 110, 26081–26088.

(21) Han, G. R.; Song, Y. J.; Jang, C. H. Label-Free Detection of Viruses on a Polymeric Surface Using Liquid Crystals. *Colloids Surf., B* **2014,** 116, 147–152.

(22) Chen, C. H.; Lin, Y. C.; Chang, H. H.; Lee, A. S. Y. Ligand-Doped Liquid Crystal Sensor System for Detecting Mercuric Ion in Aqueous Solutions. *Anal. Chem.* **2015,** 87, 4546–4551.

(23) Niu, X. F.; Liu, Y. J.; Wang, F.; Luo, D. Highly Sensitive and Selective Optical Sensor for Lead Ion Detection Based on Liquid Crystal Decorated with Dnazyme. *Opt. Express* **2019,** 27, 30421-30428.

(24) Xiang, Y.; Tong, A.; Lu, Y. Abasic Site-containing DNAzyme and Aptamer for Label-free Fluorescent Detection of Pb^{2+} and Adenosine with High Sensitivity, Selectivity, and Tunable Dynamic Range. *J. Am. Chem. Soc.* **2009,** 131, 15352-15357.

(25) Zhou, Y. Y.; Tang, L.; Zeng, G. M.; Zhang, C.; Zhang, Y.; Xie, X. Current Progress in Biosensors for Heavy Metal Ions Based on DNAzymes/DNA Molecules Functionalized Nanostructures: A review. *Sens. Actuators, B* **2016,** 223, 280-294.

(26) Jia, M.; Lu, Y. F.; Wang, R. N.; Zhang, J. L.; Xu, C. H.; Wu, J. K. Extended GR-5 DNAzyme-based Autonomous Isothermal Cascade Machine: An Efficient and Sensitive One-tube Colorimetric Platform for Pb^{2+} Detection. *Sens. Actuators, B* **2020,** 304, 127366.1-127366.7.

(27) Chu, L. T.; Leung, H. M.; Lo, P. K.; Chen, T. H. Visual Detection of Lead Ions Based on Nanoparticle-amplified Magnetophoresis and Mie Scattering. *Sens. Actuators, B* **2019,** 306, 127564.1-127564.8.

(28) Luo, J.; Xie, Z.; Lam, J. W. Y.; Cheng, L.; Chen, H.; Qiu, C.; Kwok, H. S.; Zhan, X.; Liu, Y.; Zhu, D.; Tang, B. Z. Aggregation-Induced Emission of 1-Methyl-1,2,3,4,5-Pentaphenylsilole. *Chem. Commun.* **2001,** 1740-1741.

(29) Chen, J.; Law, C. C. W.; Lam, J. W. Y.; Dong, Y.; Lo, S. M. F.; Williams, I. D.; Zhu, D.; Tang, B. Z. Synthesis, Light Emission, Nanoaggregation, and Restricted Intramolecular Rotation of 1,1-Substituted 2,3,4,5-Tetraphenylsiloles. *Chem. Mater.* **2003,** 15, 1535-1546.

(30) Mei, J.; Hong, Y.; Lam, J. W. Y.; Qin, A.; Tang, Y.; Tang, B. Z. Aggregation-Induced Emission: The Whole is More Brilliant than the Parts. *Adv. Mater.* **2014,** 26, 5429-5479.

(31) Hong, Y.; Lam, J. W. Y.; Tang, B. Z. Aggregation-Induced Emission. *Chem. Soc. Rev.* **2011,** 40, 5361-5388.

(32) Han, T. Y.; Feng, X.; Tong, B.; Shi, J. B.; Chen, L.; Zhi, J. G.; Dong, Y. P. A Novel "Turn-on'' Fluorescent Chemosensor for the Selective Detection of Al^{3+} Based on Aggregation-Induced Emission. *Chem. Commun.* **2012,** 48, 416−418.

(33) Leung, C. W. T.; Hong, Y.; Chen, S.; Zhao, E.; Lam, J. W. Y.; Tang, B. Z. A Photostable Aie Luminogen for Specific Mitochondrial Imaging and Tracking. *J. Am. Chem. Soc.* **2013,** 135, 62-65.

(34) Yuan, Y.; Zhang, C.; Liu, B. A. A Photoactivatable AIE Polymer for Light-Controlled Gene Delivery: Concurrent Endo/lysosomal Escape and DNA Unpacking. *Angew. Chem., Int. Ed.* **2015,** 54, 11419−11423.

(35) Hu, F.; Xu, S. D.; Liu, B. Photosensitizers with Aggregation-Induced Emission: Materials and Biomedical Applications. *Adv. Mater.* **2018,** 30, 1801350.

(36) Liu, Z. Y.; Zou, H.; Zhao, Z.; Zhang P. F.; Shan, G. G.; Kwok, R. T. K.; Lam, J. W. Y.; Zheng, L.; Tang, B. Z. Tuning Organelle Specificity and Photodynamic Therapy Efficiency by Molecular Function Design. *ACS Nano.* **2019,** 13, 11283–11293.

(37) Zhao, D. Y.; Fan, F.; Cheng, J.; Zhang, Y. L.; Wong, K. S.; Chigrinov, V. G.; Kwok, H. S.; Guo, L.; Tang, B. Z. Light-Emitting Liquid Crystal Displays Based on an Aggregation-Induced Emission Luminogen. *Adv. Opt. Mater.* **2014,** 3, 199-202.

(38) Zhao, D. Y.; Fan, F; Chigrinov, V. G.; Kwok, H. S; Tang, B. Z. Aggregate-Induced Emission in Light-Emitting Liquid Crystal Display Technology. J. Soc. Inf. Display **2015,** 23, 218-222.

(39) Zhao, D. Y.; He, H. X.; Gu, X. G.; G, L.; Wongm K. S.; Lam, J. W. Y.; Tang, B. Z. Circularly Polarized Luminescence and a Reflective Photoluminescent Chiral Nematic Liquid Crystal Display Based on an Aggregation-Induced Emission Luminogen. *Adv. Opt. Mater.* **2016,** 4, 534-539.

(40) Martins, H.; Naes, T. Multivariate Calibration. Wiley, New York, **1989.**

(41) Li, X.; Wang, G. K.; Ding, X.; Chen, Y. H.; Gou, Y. P.; Lu, Y. A Turn-on Fluorescent Sensor for Detection of Pb^{2+} Based on Graphene Oxide and G-quadruplex DNA. *Phys. Chem. Chem. Phys.* **2013,** 15, 12800–12804.

(42) Li, M.; Zhou, X. J.; Guo, S. W.; Wu, N. Q. Detection of Lead (II) with a Turn-on Fluorescent Biosensor Based on Energy Transfer from CdSe/ZnS Quantum Dots to Graphene Oxide. *Biosens. Bioelectron.* **2013,** 43,69–74.

(43) Qian, Z. S.; Shan, X. Y.; Chai, L. J.; Chen, J. R.; Feng, H. A. Fluorescent nanosensor Based on Graphene Quantum Dots-Aptamer Probe and Graphene Oxide Platform for Detection of Lead (II) Ion, *Biosens. Bioelectron.* **2015,** 68, 225–231.

(44) Niu, X. F.; Zhong, Y. B.; Chen, R.; Wang, F.; Liu, Y. J.; Luo, D. A "Turn-on" Fluorescence Sensor for Pb^{2+} Detection Based on Graphene Quantum Dots and Gold Nanoparticles. *Sens. Actuators,* B **2018,** 255, 1577–1581.

(45) Swasey, S. M.; Leal, L. E.; Lopez-Acevedo, O.; Pavlovich, J.; Gwinn, E. G. Silver (I) as DNA glue: Ag+-mediated Guanine Pairing Revealed by Removing Watson-Crick Constraints. *Sci. Rep.* **2015,** 5, 10163.

Table of Contents